6532 *Biochemistry* **2009,** *48,* 6532–6539
DOI: 10.1021/bi900693s

BIOCHEMISTRY
including biophysical chemistry & molecular biology
Article

Metal Binding and Activity of Ribonucleotide Reductase Protein R2 Mutants: Conditions for Formation of the Mixed Manganese−Iron Cofactor[†]

Ana Popović-Bijelić,[‡] Nina Voevodskaya,[‡] Vladimir Domkin,[§] Lars Thelander,[§] and Astrid Gräslund*[,‡]

[‡]*Department of Biochemistry and Biophysics, Stockholm University, S-10691 Stockholm, Sweden, and* [§]*Department of Medical Biochemistry and Biophysics, Umeå University, S-90187 Umeå, Sweden*

Received April 22, 2009; Revised Manuscript Received May 20, 2009

ABSTRACT: Class Ic ribonucleotide reductase (RNR) from *Chlamydia trachomatis* (*C. tm.*) lacks the tyrosyl radical and uses a Mn(IV)−Fe(III) cluster for cysteinyl radical initiation in the large subunit. Here we investigated and compared the metal content and specific activity of the *C. tm.* wild-type R2 protein and its F127Y mutant, as well as the native mouse R2 protein and its Y177F mutant, all produced as recombinant proteins in *Escherichia coli*. Our results indicate that the affinity of the RNR R2 proteins for binding metals is determined by the nature of one specific residue in the vicinity of the dimetal site, namely the one that carries the tyrosyl radical in class Ia and Ib R2 proteins. In mouse R2, this tyrosyl residue is crucial for the activity of the enzyme, but in *C. tm.*, the corresponding phenylalanine plays no obvious role in activation or catalysis. However, for the *C. tm.* wild-type R2 protein to bind Mn and gain high specific activity, there seems to be a strong preference for F over Y at this position. In studies of mouse RNR, we find that the native R2 protein does not bind Mn whereas its Y177F mutant incorporates a significant amount of Mn and exhibits 1.4% of native mouse RNR activity. The observation suggests that a manganese−iron cofactor is associated with the weak activity in this protein.

Ribonucleotide reductase (RNR)[1] catalyzes the first step in DNA precursor synthesis and provides the cell with a balanced supply of all four deoxyribonucleotides (*1*). Class I RNRs are oxygen-dependent tetrameric enzymes. The substrate binding active site is located in the large homodimer, called the R1 protein. The small homodimer (R2 protein) contains a site for a diiron cluster in each polypeptide chain. In the active form, class Ia and Ib R2 proteins contain a stable tyrosyl radical needed for catalysis (*2*, *3*). The tyrosyl radical is generated by the reductive cleavage of molecular oxygen at the diiron site in the R2 protein and is transferred to the active site in the R1 protein via a long-range radical transfer pathway (*4*). Class Ic R2 proteins lack this radical-harboring tyrosine and instead have a phenylalanine residue in the corresponding location (*5*). RNR from the bacterium *Chlamydia trachomatis* (*C. tm.*) belongs to class Ic. The reported crystal structure of the *C. tm.* R2 protein shows that in addition to the absence of the otherwise conserved radical-harboring tyrosine, the first-shell coordination sphere around the dimetal site displays interesting differences compared to class Ia and Ib R2s (*5*). In class Ic, the Fe atoms are coordinated by two histidines and four glutamates like in methane monooxygenase, instead of three glutamates and one aspartate in class Ia and Ib R2 proteins.

It has been shown that *C. tm.* protein R2 can bind manganese in the place of one iron ion and form a mixed metal Mn−Fe cluster (*6*, *7*). Furthermore, enzyme activity measurements and Mössbauer spectroscopy indicated that *C. tm.* RNR uses a stable Mn(IV)−Fe(III) cofactor for cysteinyl radical initiation in R1 (*6*). The manganese- and iron-containing wild-type *C. tm.* R2 protein shows considerably higher specific activity (∼6-fold) than its iron-only counterpart (*7*).

It has recently been shown, by density functional theory calculations, that the Mn(IV) ion of the Mn(IV)−Fe(III) cofactor is an equally strong oxidant as a tyrosyl radical in class Ia *Escherichia coli* R2 protein (*8*). This property may be important for the reversible electron transfer associated with efficient RNR catalysis. In contrast, the calculations showed that the corresponding diiron form of the cofactor, Fe(III)−Fe(IV), would have a much higher redox potential and therefore be a stronger oxidant. This might hinder the reversible electron transfer and require that the Fe(III)−Fe(IV) active state of the enzyme be created anew by reduction and reaction with molecular oxygen in each catalytic cycle. This in turn could be the reason for the slow enzymatic reaction accomplished with this form of the cofactor (*7*−*9*).

Recently, the metal−metal distances in different oxidation states of the mixed metal Mn−Fe cofactor have been determined (*10*): 4.15 Å for Mn(II)−Fe(II), 3.25 Å for Mn(III)−Fe(II), 2.90 Å for Mn(III)−Fe(III), and 2.75 Å (2.92 Å reported in ref (*11*)) for Mn(IV)−Fe(III). The short distance calculated

[†]This study was supported by a grant from the Swedish Research Council.

*To whom correspondence should be addressed: Department of Biochemistry and Biophysics, The Arrhenius Laboratories for Natural Sciences, Stockholm University, SE-106 91 Stockholm, Sweden. Phone: +46 8 16 2455. Fax: +46 8 153679. E-mail: astrid@dbb.su.se.

[1]Abbreviations: RNR, ribonucleotide reductase; *C. tm.*, *Chlamydia trachomatis*; pp, polypeptide chain; EPR, electron paramagnetic resonance spectroscopy; CDP, cytidine 5′-diphosphate; DTT, dithiothreitol; *A*, hyperfine coupling (hfc) constant; *D* and *E*, axial and rhombic zero field splitting (ZFS) constants, respectively.

 Published on Web 06/03/2009

for the high-valent Mn(IV)−Fe(III) state suggests a tribridged μ-oxo/μ-hydroxo/μ-carboxylato core structure (*11*).

Because of the crucial function of the metal cofactor in catalysis involving class I RNRs, we decided to investigate what other factors, besides iron and/or manganese availability, may regulate the metal binding in the cofactor. One important question concerns the role of the phenylalanine residue in class Ic RNR (F127 in *C. tm.*), which corresponds to the radical-forming residue in class Ia and Ib RNRs (Y177 in mouse and Y122 in *E. coli*). In the latter two, the residue is essential for the enzyme activity, yet in *C. tm.* RNR, it plays no role in the activation or the catalysis pathway (*12*). Therefore, we have investigated the metal uptake and enzyme activity in *C. tm.* wild-type protein R2 and its F127Y mutant. The Y129F R2 mutant was included as a control. For the comparison of the role of the radical-forming residue in metal binding, we performed similar measurements for the class Ia native mouse protein R2 and its Y177F mutant.

MATERIALS AND METHODS

Expression and Purification of RNR Proteins. *C. tm.* proteins were overexpressed in *E. coli* BL21(DE3) bacteria containing pET3a-R2 plasmids encoding native and mutant R2 proteins F127Y and Y129F and plasmid pET3a-CTR1Δ1−248 encoding the truncated wild-type R1 protein. Mouse proteins were overexpressed in Rosetta 2(DE3)pLysS bacteria containing pET-R2 plasmids encoding native and mutant mouse R2 protein Y177F. The bacteria were grown in LB medium (with and without metal supplement) at 37 °C until they reached an A_{595} of 0.8 and then induced with 500 μM isopropyl 1-thio-β-D-galactopyranoside (IPTG) and grown for an additional 20 h at 17 °C before being harvested. For cells grown in manganese-enriched LB medium, 80 μM $MnCl_2$ was gradually added after induction with IPTG (*10*). *C. tm.* RNR proteins were purified as described by Roschik *et al.* (*13*) and mouse R2 proteins as described by Mann *et al.* (*14*). Mouse R2 apoprotein was obtained using the same procedure except all buffers contained 1 mM EDTA and 10 μM phenylmethanesulfonyl fluoride. Mouse R1 protein was expressed and purified as described by Davis *et al.* (*15*).

Reconstitution Reaction of Mouse R2 Proteins. Reconstitution of the metal site in R2 protein was accomplished prior to the activity assay. The oxygen-saturated apoprotein was incubated with an equal volume of $MnCl_2$ solution (3-fold molar excess) for 20 min on ice. A 6-fold molar excess of an anaerobic $(NH_4)_2Fe(SO_4)_2$ solution (Mohr's salt) was added. After incubation for 30 min on ice, excess iron and manganese were removed by gel filtration.

Metal Content Determination. The iron content of all proteins was spectrophotometrically determined using an iron/TIBC (ferrozine) reagent set from Eagle Diagnostics. Manganese content was determined in acid-denatured proteins by EPR spectroscopy at 293 K with a microwave power of 3 mW and a modulation amplitude of 1 mT. The concentration of manganese was determined from the amplitude of the EPR signal and compared with a standard solution of 0.5 mM $MnCl_2$ (*10*). Metal content was confirmed by total reflection X-ray fluorescence spectroscopy (TXRF) on a Bruker S2 Picofox spectrometer.

Ribonucleotide Reductase Activity Assay. Ribonucleotide reductase R2 activity was determined from the rate of reduction of [^{3}H]CDP. One unit is defined as the amount of enzyme which, in the presence of excess R1 subunit, catalyzes the formation of 1 nmol of dCDP per minute at 37 °C (*16*). The following reagents were incubated at 37 °C for 20 min in a final volume of 50 μL: 2 μM R2, 10 μM R1, 4 mM [^{3}H]CDP (specific activity, 10500 cpm/nmol), 10 mM dithiothreitol (DTT), 50 mM KCl, 0.4 mM ATP, 6.4 mM $MgCl_2$, 0.01 mM $FeCl_3$, and 40 mM Hepes buffer (pH 7.5). The recovery of the dCMP carrier was ~95%.

Sample Preparation for Electron Paramagnetic Resonance Spectroscopy. The reduced form of *C. tm.* Y129F R2 protein was prepared by incubation of 120 μM protein with 30 mM sodium dithionite for 2 min at 298 K. The Fe(III)−Mn(III) state of the *C. tm.* Y129F R2 protein was prepared by incubation of 120 μM protein with 12 mM DTT for 5 min at 298 K. All samples were manually frozen in cold isopentane.

Electron Paramagnetic Resonance Spectroscopy. EPR spectra (9.5 GHz) were recorded on a Bruker ESP 300 X-band spectrometer with an Oxford Instruments ESR9 helium cryostat as described previously (*7*, *17*). All spectra were recorded at 20 K with a microwave power of 3 mW and a modulation amplitude of 0.5 mT. The spectra were simulated using EasySpin, a computational package for spectral simulation based on Matlab (*18*).

RESULTS

In this study, we have investigated the affinity of RNR in binding different metals and forming mixed metal clusters in *C. tm.* wild-type protein R2 and its F127Y mutant. We investigated the extent to which the mixed metal cluster would be formed in these R2 proteins depending on metal availability; if there is a "natural" affinity of the protein for either metal, perhaps determined by its structure; and, finally, if the formation of a mixed metal cofactor is related to an increased specific activity of the protein, as is the case for *C. tm.* wild-type R2. The *C. tm.* Y129F R2 mutant was included in this study as a control and also because it had been reported to be essentially enzymatically inactive (*13*), and we investigated if this was due to its metal uptake.

In parallel, class Ia native mouse protein R2 and its Y177F mutant were investigated using the same protocols. We studied whether the Mn−Fe cofactor can also be formed in the native or mutant mouse R2 protein and, if so, whether it will affect enzymatic activity.

C. tm. RNR. *C. tm.* wild-type R2 and the F127Y and Y129F mutant proteins were purified from bacterial cells grown under two conditions: in the standard LB medium, in which the iron concentration was 8 μM and manganese concentration was less than 0.05 μM, and in a Mn-enriched medium, in which the Fe concentration was the same but the concentration of Mn was approximately 30 μM. After purification, the proteins were assayed for metal content and specific activity (Table 1). It is seen that when cells were grown in Mn-enriched LB medium, both wild-type and Y129F R2 incorporated comparable amounts of Fe and Mn, whereas F127Y R2 had a much lower content of Mn than Fe (0.04 Mn/pp compared to 0.45 Fe/pp). When cells were grown in normal LB medium, the level of Mn incorporation was at least 10-fold lower than that of Fe for all three proteins.

Next, the specific activities of the three proteins produced in cells grown under high- and low-Mn conditions were compared. As expected, the *C. tm.* wild-type protein grown with Mn exhibits significantly higher specific activity (180 units) than its low-Mn-containing counterpart (30 units) (*7*). For the two mutants, we observed the following (Table 1): Only F127Y R2 has any

Table 1: Specific Activities and Metal Contents of *C. tm.* RNR R2 Proteins[a]

protein	specific activity [nmol (mg of R2)$^{-1}$ min^{-1}]	metal content[b] Fe/pp	metal content[b] Mn/pp
wild-type R2[c]	30 ± 5	0.600 ± 0.030	0.057 ± 0.003
wild-type R2 (grown with Mn)[d]	180 ± 20	0.570 ± 0.030	0.450 ± 0.020
wild-type R2 (grown with Mn)[e]	120 ± 10	0.980 ± 0.030	0.290 ± 0.010
wild-type R2 (grown with Mn), anaerobic[e,f]	80 ± 5	0.980 ± 0.030	0.290 ± 0.010
F127Y R2[c]	21 ± 3	0.470 ± 0.020	0.014 ± 0.001
F127Y R2 (grown with Mn)[d]	22 ± 3	0.450 ± 0.020	0.042 ± 0.001
F127Y R2, anaerobic[c,f]	2.0 ± 0.5	0.470 ± 0.020	0.014 ± 0.001
Y129F R2[c]	0.2 ± 0.1	0.410 ± 0.020	0.005 ± 0.001
Y129F R2 (grown with Mn)[d]	0.2 ± 0.1	0.320 ± 0.020	0.270 ± 0.010

[a] The proteins were purified and investigated with no further treatment. [b] Metal content is given per polypeptide chain (pp). [c] Protein was purified from bacteria grown in LB medium: initial Fe concentration was 8 μM and Mn concentration was ≤0.05 μM. [d] Protein was purified from bacteria grown in manganese-enriched LB medium: initial Fe concentration was 8 μM and Mn concentration was 30 μM. [e] Different preparation of the protein purified from bacteria grown in Mn-enriched LB medium. [f] Activity assay performed under anaerobic conditions: the assay mixture contained 1.5 μg/mL rat liver mitochondrial protein and 2 μM cytochrome *c*.

significant activity (21−22 units), which however does not correlate with the Mn content which is low (0.01−0.04 Mn/pp) and independent of growth conditions. This low activity, also reported in ref (*13*), is comparable with that of the low-Mn wild-type R2 and may also be caused by the redox activity of the diiron site. The activity of F127Y R2 is essentially lost (down to 2 units from 22 units) when the assay is performed under anaerobic conditions, which indicates that oxygen is required for catalysis. The activity of the manganese-containing wild-type R2 is decreased from 120 to 80 units under the same anaerobic conditions (Table 1), indicating that catalysis is only partially sensitive to the presence of oxygen. Y129F R2 is devoid of enzymatic activity, independent of whether it has bound a significant amount of Mn.

Since the assayed R2 proteins presented in Table 1 had relatively low metal content directly after purification, eight different concentrations of Fe and Mn (in the range of 0.01−0.05 mM Fe and 0.05−0.1 mM Mn) were added to the activity assay mixtures, to see if this would increase the observed specific activities. A 2-fold increase was observed only in low-Mn-containing wild-type *C. tm.* R2 [from 30 to 60 units (data not shown)], which indicates that the protein could incorporate some of the Mn from the assay mixture.

EPR Spectroscopy. Low-temperature X-band EPR spectra from Mn(II) ions in different buffers are to some extent variable (Figure S1, Supporting Information). Depending on the nature of the ligands, both spectral intensity and hyperfine couplings can vary. In acetate and phosphate buffer, the EPR spectrum at 20 K shows the typical high-spin ($^5/_2$) Mn(II) six hyperfine lines centered at $g = 2$, characteristic of the central fine structure transition ($-^1/_2 \leftrightarrow {}^1/_2$). In these buffers, Mn is octahedrally coordinated to oxygen ligands exhibiting a hyperfine coupling constant of 260 MHz (95 G) (*19*). The corresponding spectrum in Tris-HCl buffer is similar but has a much lower line intensity.

The X-band EPR spectra of *C. tm.* RNR R2 proteins from cells grown in Mn-enriched medium are shown in Figure 1. The proteins were collected directly after purification with no further treatment. They were dissolved in Tris buffer (pH 7.6), and the spectra were recorded at 20 K. The two R2 proteins, *C. tm.* wild-type and Y129F R2, which had incorporated significant amounts of Mn (Table 1), exhibit EPR signals characteristic of high-spin Mn(II) ions (Figure 1 a,b) similar to the EPR signals observed in acetate and phosphate buffer (Figure S1, Supporting Information). The five higher-field hyperfine transitions give a visible three-peak pattern which is attributed to the forbidden transitions ($\Delta M_S = \pm 1, \Delta M_I = \pm 1$). They are caused by second-order (time-independent) effects due to cross products of the electron and nuclear spin operators and are common for protein-bound Mn(II) (*20*, *21*). The $g \sim 2.2$ signal (marked with an arrow) in the spectra of wild-type and Y129F R2 as-purified proteins is characteristic of the antiferromagnetically coupled Mn(III)−Fe(III) state in R2 (*10*). Its appearance indicates that the protein that emerges from the purification process contains a fraction of Mn coupled to Fe, in addition to the uncoupled Mn(II) ions.

Strong reduction of Y129F R2 with sodium dithionite gives the result that apparently all manganese is reduced to Mn(II). The resulting EPR spectrum lacks the $g \sim 2.2$ signal and exhibits a Mn(II) signal twice as large as that of the as-purified protein (Figure 1c). Quantitatively, this signal corresponds to almost all manganese present in the sample (data not shown).

Milder reduction procedures of the as-isolated Y129F R2 in the presence of oxygen give rise to higher metal oxidation states. Reduction with DTT gives rise to the Mn(III)−Fe(III) ($S = {}^1/_2$) and Mn(IV)−Fe(III) ($S = 1$) states (Figure 1d). In this case, all manganese is apparently oxidized and forms coupled sites with iron ions. The quantification of the EPR visible $S = {}^1/_2$ signal presented in Figure 1d reveals that the contribution of the Mn(III)−Fe(III) state is only ∼0.05 per dimer, which corresponds to ∼7.5% of all Mn in the sample. The rest is invisible, and we conclude that more than 90% of the manganese is in the $S = 1$ EPR invisible Mn(IV)−Fe(III) state.

The EPR spectra of the protein-bound Mn(II) and Mn(III)−Fe(III) states in Y129F R2 can be simulated (Fig 1 f,g), using parameters listed in Table 2 (simulations I and II, respectively). The EPR signal from the Mn(III)−Fe(III) state formed in the *C. tm.* wild-type R1/R2 holoenzyme (*7*) is different from that formed in the Y129F R2 protein alone. The holoenzyme spectrum is broader (700 G) and can be simulated (Figure 1h) with a different set of $A(^{55}\text{Mn})$ values (Table 2, simulation III). This indicates that the covalency of metal−ligand bonds of this coupled state is changed when it is formed only in the R2 subunit or in the complex (*19*−*21*).

The EPR spectrum of the F127Y R2 protein from cells grown in manganese-enriched medium (Figure 1e) exhibits a low-intensity signal that is characteristic of Mn(II) ions dissolved

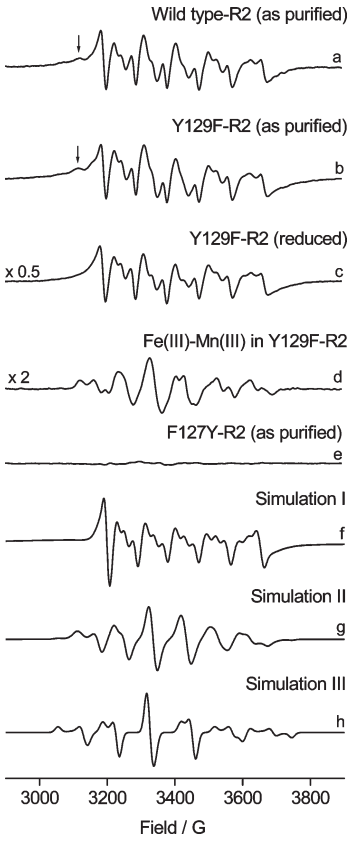

FIGURE 1: EPR spectra of *C. tm.* RNR R2 proteins from cells grown in manganese-enriched medium at 20 ± 0.4 K. (a) Wild-type R2 (as purified), 0.45 Mn/pp, 0.57 Fe/pp. (b) Y129F R2 mutant (as purified), 0.27 Mn/pp, 0.32 Fe/pp. (c) Y129F R2 mutant reduced with sodium dithionite, 0.27 Mn/pp, 0.32 Fe/pp. (d) Mn(III)−Fe(III) state in Y129F R2, 0.27 Mn/pp, 0.32 Fe/pp. (e) F127Y R2 mutant (as purified), 0.04 Mn/pp, 0.45 Fe/pp. (f) Simulation of the experimental spectrum shown as spectrum c, from Mn(II) ions in reduced Y129F R2 ($S = {}^5/_2$, $g = 2$, $A = 260$ MHz, $D = 490$ MHz, $E/D = 0.2$, D strain = 400 MHz, $\Delta H = 42$ MHz). (g) Simulation of the experimental spectrum shown as spectrum d, from the Mn(III)−Fe(III) state formed in Y129F R2 [$S = {}^1/_2$, g = [2.015, 2.025, 2.02], $A(^{55}\text{Mn})$ = [250, 230, 320] MHz, $A(^{56}\text{Fe})$ = [62, 67, 65] MHz, $\Delta H = 50$ MHz]. (h) Simulation of the experimental spectrum from the Mn(III)−Fe(III) state formed in the wild-type R1/R2 holoenzyme [$S = {}^1/_2$, g = [2.015, 2.009, 2.024], $A(^{55}\text{Mn})$ = [390, 315, 270] MHz, $A(^{56}\text{Fe})$ = [67, 70, 62] MHz, $\Delta H = 50$ MHz]. All experimental spectra are appropriately scaled to show the relative intensities of signals. The spectrum of $MnCl_2$ in Tris-HCl buffer has been subtracted from all spectra (except from spectrum e).

in Tris-HCl buffer, which indicates that Mn is unspecifically bound on the protein. Upon incubation with a reductant, DTT or sodium dithionite, the spectrum is unchanged. In the reaction with the complete catalytic mixture containing R1, CDP, ATP, DTT, $MgCl_2$, $FeCl_3$, and KCl, an EPR signal characteristic of the Fe(III)−Fe(IV) state is formed (spectrum not shown), as previously reported in ref (*22*).[2] The Fe(III)−Fe(IV) EPR signal decayed ~50% over a period of 3 h at room temperature but did not give rise to any detectable tyrosyl radical signal (data not shown).

Mouse RNR. Recombinant mouse native and mutant Y177F R2 proteins were grown in *E. coli* cells under conditions of low and high Mn concentrations in the medium. In Y177F R2 under high-Mn growth conditions, Mn became incorporated into the protein to approximately the same extent as Fe (Table 3). In contrast, under the same growth conditions, native mouse R2 had 6-fold less Mn than Fe. Specific activities were low for native R2 grown with Mn and for Y177F R2 independent of Mn incorporation. Only the native R2 protein purified from cells grown under regular (low Mn) conditions had the normal specific activity.

We then turned to metal reconstitution experiments with these proteins. After reconstitution with manganese and anaerobic iron, Y177F R2 and the native mouse R2 protein incorporated similar amounts of Fe [1.5 and 1.2 Fe/pp, respectively (Table 3)]. However, under the same reconstitution conditions, Y177F R2 incorporated significant amounts of Mn [0.5 Mn/pp (Table 3)] whereas the native mouse R2 protein incorporated only 0.02 Mn/pp.

The Mn- and Fe-reconstituted Y177F R2 protein exhibited 1.4±0.4% of native mouse activity (2.1 compared to 150 units, Table 3). To rule out the possibility that this small activity was not due to contamination with host RNR, the assay was repeated using another R1 subunit, *C. tm.* instead of mouse R1, and also in the presence of two different C-terminal inhibitory peptides for mouse RNR (*23*), N-Ac-NSFTLDADF and N-Ac-VISNSTENSFTLDADF. Such peptides are based on the species-specific C-terminal sequences of protein R2 which are known to specifically inhibit RNR enzymes due to competitive binding to R1. In all these cases, the reconstituted mouse Y177F R2 lost its specific activity (at least 10-fold lower than that observed with mouse R1 in the absence of inhibitors). The fact that no tyrosyl radical could be detected in the samples also supported the conclusion that there was no contamination with host R2.

The weak activity of native mouse R2 from cells grown in Mn-enriched medium can be attributed to the low iron (and hence low tyrosyl radical) content. However, it was possible to reconstitute this protein with anaerobic iron and increase its activity almost 200 times (to 120 units).

EPR spectra of the reconstituted and non-reconstituted mouse Y177F R2 proteins (Figure 2 a,b) are different in terms of line broadening. These two preparations of the protein differ only in the metal content: reconstituted Y177F R2 has fully occupied metal sites with 0.5 Mn/pp and 1.5 Fe/pp, while the non-reconstituted protein has only partially filled metal sites, 0.24 Mn/pp and 0.23 Fe/pp. Both spectra can be simulated for a ^{55}Mn(II) system with $S = {}^5/_2$, $g = 2$, and $A = 260$ MHz and different ZFS constants (simulations I and IV, Table 2).

Our attempts to observe the EPR signals from the Mn(III)−Fe(III) and Mn(IV)−Fe(IV) states obtained from the mild reduction or reactivation with hydrogen peroxide of reconstituted mouse Y177F R2 have not been conclusive, neither in the R2 subunit alone nor in the R1/R2 holoenzyme. We believe that one reason for this is that the dimetal site in the mouse R2 protein is more exposed to external agents than in *C. tm.* or *E. coli* proteins (*24*). As soon as any kind of reductant is added (DTT, sodium dithionite, or Fe(II) ions which were used for reconstitution), the metals are reduced, become much more labile, and are easily lost from the protein (*25*). The only visible EPR signals arise from unbound manganese ions in Tris-HCl buffer.

DISCUSSION

C . tm. RNR. F127Y R2 protein does not bind Mn when cells are grown in the Mn-enriched medium but shows low activity comparable to that of low-Mn containing wild-type R2.

[2]The Fe(III)−Fe(IV) EPR signal is unstable during storage in liquid nitrogen and decreases in intensity by ~30% per 24 h storage. That could explain the failure to observe it as reported in ref (*6*).

Table 2: Simulation Parameters for EPR Spectra of RNR R2 Proteins

simulation I[a]	simulation II[b]	simulation III[c]	simulation IV[d]
$S = {}^5/_2$	$S = {}^1/_2$	$S = {}^1/_2$	$S = {}^5/_2$
$g = 2$	$g = [2.015, 2.025, 2.02]$	$g = [2.015, 2.009, 2.024]$	$g = 2$
$A(^{55}\text{Mn}) = 260$ MHz	$A(^{55}\text{Mn}) = [250, 230, 320]$ MHz	$A(^{55}\text{Mn}) = [390, 315, 270]$ MHz	$A(^{55}\text{Mn}) = 260$ MHz
$D = 490$ MHz	$A(^{56}\text{Fe}) = [62, 67, 65]$ MHz	$A(^{56}\text{Fe}) = [67, 70, 62]$ MHz	190 MHz $\leq D \leq$ 320 MHz
D strain $= 400$ MHz	$\Delta H = 50$ MHz	$\Delta H = 50$ MHz	120 MHz $\leq D$ strain $\leq$ 250 MHz
$0.19 \leq E/D \leq 0.27$			$0 \leq E/D \leq 0.3$
$\Delta H = 42$ MHz			$\Delta H = 28$ MHz

[a] Protein-bound Mn(II) in *C. tm.* wild-type R2, Y129F R2, and non-reconstituted mouse Y177F R2. [b] Mn(III)−Fe(III) state in *C. tm.* Y129F R2. [c] Mn(III)−Fe(III) state in the *C. tm.* wild-type R1/R2 complex. [d] Protein-bound Mn(II) in reconstituted mouse Y177F R2 (0.5 Mn/pp and 1.5 Fe/pp).

Table 3: Specific Activities and Metal Contents of Mouse RNR R2 Proteins

protein	specific activity [nmol (mg of R2)$^{-1}$ min^{-1}]	metal content[a]	
		Fe/pp	Mn/pp
native mR2[b] (0.2 Tyr$^\bullet$/pp)	100 ± 5	0.57 ± 0.03	0.010 ± 0.005
native mR2 (grown with Mn)[c] (0.04 Tyr$^\bullet$/pp)	0.4 ± 0.1	0.24 ± 0.01	0.04 ± 0.01
reconstituted (Fe) native mR2[d] (0.33 Tyr$^\bullet$/pp)	120 ± 5	1.00 ± 0.1	0.010 ± 0.005
reconstituted (Mn and Fe) native apo-mR2[e] (0.4 Tyr$^\bullet$/pp)	150 ± 9	1.20 ± 0.1	0.02 ± 0.01
mY177F R2[b]	0.10 ± 0.05	0.23 ± 0.02	0.05 ± 0.01
mY177F R2 (grown with Mn)[c]	0.10 ± 0.05	0.23 ± 0.02	0.24 ± 0.02
reconstituted (Mn and Fe) mY177F-R2[f]			
in the presence of mouse R1	2.1 ± 0.6	1.50 ± 0.15	0.50 ± 0.05
in the presence of *C. tm.* R1	0.2 ± 0.1	1.50 ± 0.15	0.50 ± 0.05
in the presence of N-Ac-NSFTLDADF	≤ 0.1	1.50 ± 0.15	0.50 ± 0.05
in the presence of N-Ac-VISNSTENSFTLDADF	≤ 0.1	1.50 ± 0.15	0.50 ± 0.05

[a] Metal content is given per polypeptide chain (pp). [b] Protein was purified from bacteria grown in LB medium: initial Fe concentration was 8 μM and Mn concentration was $\leq$0.05 μM. [c] Protein was purified from bacteria grown in Mn-enriched LB medium: initial Fe concentration was 8 μM and Mn concentration was 30 μM. [d] Protein was purified from bacteria grown in Mn-enriched LB medium and reconstituted with a 6-fold molar excess of an anaerobic $(NH_4)_2Fe(SO_4)_2$ solution. [e] Apoprotein was purified from bacteria grown in regular LB medium and reconstituted with a 3-fold molar excess of $MnCl_2$ and 6-fold molar excess of an anaerobic $(NH_4)_2Fe(SO_4)_2$ solution. [f] Protein was purified from bacteria grown in regular LB medium and reconstituted with a 3-fold molar excess of $MnCl_2$ and a 6-fold molar excess of an anaerobic $(NH_4)_2Fe(SO_4)_2$ solution.

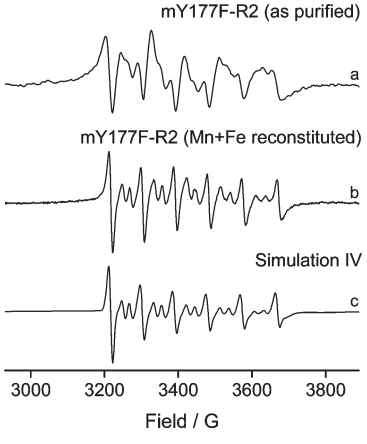

FIGURE 2: EPR spectra of the mouse Y177F R2 mutant protein from cells grown in manganese-enriched medium at 20 ± 0.4 K. (a) Non-reconstituted (as purified) Y177F R2, with 0.24 Mn/pp and 0.23 Fe/pp. (b) Y177F R2 reconstituted with manganese and iron, with 0.50 Mn/pp and 1.50 Fe/pp. (c) Simulation of the experimental spectrum shown in b, from Mn(II) ions in reconstituted Y177F R2 ($S = {}^5/_2$, $g = 2$, $A = 260$ MHz, $D = 250$ MHz, $E/D = 0$, and $\Delta H = 28$ MHz).

Despite the presence of the Y127 residue we could not observe any significant amount of stable tyrosyl radical in this protein. The enzyme activity is independent of the Mn content of the protein and is lost in the absence of oxygen. Thus, we suggest that this small activity may be due to the formation of the Fe(III)−Fe(IV) state as proposed before for low-Mn containing wild-type R2 (*7*). The oxygen dependence results further suggest that the diiron cluster may only function for one half-cycle in the RNR catalysis. A reason could be that the difference between the redox potentials of the metal cluster in R2 and the cysteine residue in R1 must be rather small to yield reversible electron transfer between the two sites during one catalytic cycle. The reversible transfer, which should be controlled by the protein system, is obviously functional for R2s with tyrosyl radical (*26*) as well as with Mn(IV)−Fe(III) cofactor (see Table 1). Since the Fe(III)−Fe(IV) cluster is a much stronger oxidant than the Mn(IV)−Fe(III) cluster (*8*), it is likely that in the active state the electron is transferred only one way from R1 to R2, but not back to R1. The next turnover may then be performed only after the reduction and reoxygenation of the dimetal site with molecular oxygen.

Our results also show evidence (Table 1) that when oxygen is removed from the activity assay mixture of manganese-containing *C. tm.* wild-type R2, the specific activity is reduced by only 30% during the 20 min anaerobic assay reaction. This indicates that the Mn(IV)−Fe(III) cofactor functions reversibly in many catalytic cycles in the absence of oxygen, although the presence of oxygen is obviously needed for the reactivation of the cofactor at certain intervals during the time of the assay.

In agreement with previous observations (*13*), Y129F R2 exhibits no enzymatic activity, even upon binding of Mn. When incubated with a mild reductant, DTT, in the presence of O_2, the subunit is activated and forms the coupled Mn(III)−Fe(III) state.

This state is different from that formed in the R1/R2 holoenzyme (in *C. tm.* wild type) and is assigned to the coupled state formed only in R2 (*10*). When DTT is added to Y129F R2 incubated with R1 or the complete catalytic mixture (R1, CDP, ATP, DTT, $MgCl_2$, $FeCl_3$, and KCl), the EPR signal does not change from that shown in Figure 1d. The existence of the coupled state in R2 proves that the subunit can be activated and is not responsible for the lack of enzymatic activity of this mutant. The fact that the addition of R1 (or the complete catalytic mixture) makes no change in the EPR spectrum suggests that the active R1/R2 complex is not formed in this mutant. There are two explanations: residue 129 is part of either the catalysis-specific electron transfer pathway or the binding interface between R1 and R2 subunits. Since it was previously shown that the catalysis pathway does not include this residue (*12*), we suggest that residue Y129 of *C. tm.* wild-type R2, located on the surface of the protein (*5*), is involved in the binding of the R1 and R2 subunits.

Mouse RNR. When bacterial cells are grown in Mn-enriched medium, the phenylalanine-containing mouse mutant, Y177F R2, binds Mn as opposed to the tyrosine-containing native R2 protein. The reports on the specific activity of mouse Y177F R2 have been contradictory. It has been shown that when the apoprotein of this mutant is reconstituted with only iron it is essentially enzymatically inactive (0.1% of native activity) (*27*). On the other hand, an early report by the Cooperman group had shown that this mutant had 0.5% of native activity, which furthermore could be inhibited by a specific C-terminal heptapeptide, N-Ac-FTLDADF (*28*). Our preparation of Y177F R2 reconstituted with Mn and anaerobic Fe, which gave metal contents of 0.5 Mn/pp and 1.5 Fe/pp, exhibited 1.4% of native mouse activity (Table 3). This activity could be inhibited by two mouse-specific C-terminal peptides ("9-mer" and "16-mer"). We suggest that the low activity observed here may be the result of the formation of the active Mn(IV)−Fe(III) cluster, which is able to replace the tyrosyl radical needed for radical initiation in R1. There is a possibility that the mutant activity reported previously (*28*) could be due to a small Mn contribution to the cofactor in that R2 protein.

EPR Spectra of Manganese-Containing RNR Proteins. *C. tm.* wild-type R2, Y129F R2, and mouse Y177F R2 as-purified proteins exhibit very similar EPR spectra. The spectra of *C. tm.* R2s show significant contributions from the Mn(III)−Fe(III) state (marked with an arrow in Figure 1a,b) in addition to the signal from protein-bound Mn(II) ions. From additions of simulated EPR spectra (Figure 1f,g), we could estimate the contribution of the Mn(III)−Fe(III) spectrum to be ∼20% in these cases (data not shown). The EPR spectrum of mouse Y177F R2 is also dominated by a Mn(II) signal and in addition shows a weak contribution from a second spectral component which may be the Mn(III)−Fe(III) signal. Although not conclusive, an added simulation (of spectra in Figure 1f,g) suggests that ∼10% of the Mn(III)−Fe(III) signal may contribute here (data not shown). In all three proteins, the Mn(II) EPR signal can be simulated for a system with $S = {}^5/_2$, $g = 2$, and $A =$ 260 MHz and different ZFS constants. The relative magnitudes of ZFS parameters give information regarding the metal−ligand coordination strength and geometry (*29*) and are extremely sensitive to the nature of the ligands (*30*). For reconstituted mouse Y177F R2, the values of D are in the range of 190−320 MHz, which indicates regular octahedral symmetry for Mn ions bound in R2 (*31*). The value of D for non-reconstituted mouse Y177F R2 and *C. tm.* wild type and Y129F R2 is found to be 490 MHz. The increased value of D is the result of a slight distortion from the octahedral symmetry. These spectra also exhibit line broadenings which are caused by small variations in metal−ligand coordination resulting from different Mn(II) ions having different D values (*32*). The variations are simulated with the D strain (Gaussian distribution of the D parameter). Similar values of D have been reported for other Mn-containing proteins [200 MHz for concanavalin A (*20*), 330 MHz for the G protein Ras p21, 900 MHz for Mn metalloglutathione transferase FosA (*33*), 340 MHz for cytochrome *c* oxidase (*34*), and 690 MHz for oxalate decarboxylase (*35*)].

Manganese Binding in RNR Proteins. The R2 proteins studied here may be divided into two groups with respect to the residue located next to the dimetal site. The first group comprises *C. tm.* wild-type R2, Y129F R2, and mouse Y177F R2 proteins, all of which contain a phenylalanine in this position. The second group, consisting of *C. tm.* F127Y R2 and native mouse R2 proteins, has a tyrosine close to the metal site. Our experiments show that when cells are grown in the Mn-enriched medium, the proteins from the first group bind Mn in one metal site while the proteins from the second group prefer only Fe. It seems that the protein's affinity for metals is altered by the replacement of only one specific amino acid residue. In mouse R2, this amino acid is crucial for the enzyme's activity, but in *C. tm.*, it plays no role in the activation or the catalysis pathway (*12*), yet it determines whether Mn will be bound instead of Fe. Selective binding of different metal ions in biological systems depends on the charge, size, and type of ligands, coordination geometry, spin-pairing stabilization, and selection by binding in clusters (*36*). This means that in proteins the amino acid ligands form cavities of particular sizes and shapes that are suitable for different metals. Furthermore, the (nonliganding) neighboring amino acids are also shown to influence the structure and stability of these sites. The role of the phenylalanine residue in the vicinity of the metal site has been studied in some Mn-containing enzymes. It is shown that the phenyl group of F216 in phosphoenolpyruvate carboxykinase from *Saccharomyces cerevisiae* provides a low-polarity microenvironment suitable for keeping lysine, one of the ligands binding the Mn(II), in the unprotonated form and that mutation of this residue results in a lower affinity of the enzyme for Mn(II) ions (*33*, *37*).

Recently, it has been shown that Mn binding in the dimetal site of *Mycobacterium tuberculosis* protein Rv0233 (an R2 class Ic-like protein) is very specific (*38*). In this case, anomalous diffraction difference maps show that the manganese ion occupies only the site closest to the position of the phenylalanine and that there is no sign of iron binding in this site. We conclude that the presence of the F127 residue close to the dimetal site of *C. tm.* RNR R2 provides adequate molecular environment properties (because of its size, shape, polarity, and/or hydrophobicity) that could increase the affinity of the enzyme for manganese ions.

CONCLUSION

The objective of this study was to improve our understanding of the structure−activity relationship of the novel dimetal active site in *C. tm.* ribonucleotide reductase. The *C. tm.* F127Y R2 mutant does not bind Mn to any significant extent and has a low specific activity comparable to that of low-Mn containing wild-type R2. The activity is lost in the absence of oxygen. These results suggest that *C. tm.* R2 in the absence of Mn is functional

for only one-half of an enzymatic cycle through the formation of the Fe(III)−Fe(IV) state.

The native mouse protein R2 does not bind manganese, whereas its Y177F mutant does. The reconstituted mouse Y177F-R2 protein exhibits 1.4% of native mouse RNR specific activity. This activity can be inhibited with mouse R2 C-terminal peptides. The results suggest that the Mn−Fe cofactor may be able to replace the tyrosyl radical needed for catalysis also in this RNR, however with a much smaller enzymatic activity.

In conclusion, our results indicate that the F127 residue instead of Y in this position, next to the dimetal site in *C. tm.* RNR R2 protein, increases the affinity of the enzyme for Mn(II) ions. The phenylalanine residue provides suitable molecular environment properties of the dimetal site possibly by affecting the p*K* values of neighboring metal−liganding amino acids. The resulting Mn−Fe form of the cofactor allows reversible electron transfer and continuous catalytic activity.

ACKNOWLEDGMENT

We thank Professor Grant McClarty (University of Manitoba, Winnipeg, MB) for his kind gift of the plasmids for *C. tm.* RNR proteins and Dr. Michael Haumann (Free University Berlin, Berlin, Germany) for providing access to TXRF. We also thank Mr. Torbjörn Astlind (Stockholm University, Stockholm, Sweden) for expert instrumental assistance.

SUPPORTING INFORMATION AVAILABLE

X-Band EPR spectra at 20 ± 0.4 K of 20 μM $MnCl_2$ in various buffers (50 mM acetate buffer at pH 4.5, 50 mM phosphate buffer at pH 7.0, and 50 mM Tris-HCl buffer at pH 7.6). This material is available free of charge via the Internet at http://pubs.acs.org.

REFERENCES

(1) Thelander, L., and Reichard, P. (1979) Ribonucleotide reductase. *Annu. Rev. Biochem. 48*, 133–158.
(2) Sjöberg, B.-M., Reichard, P., Gräslund, A., and Ehrenberg, A. (1978) The tyrosine free radical in ribonucleotide reductase from *Escherichia coli*. *J. Biol. Chem. 253*, 6863–6865.
(3) Gräslund, A., and Sahlin, M. (1996) Electron paramagnetic resonance and muclear magnetic resonance studies of class I ribonucleotide reductase. *Annu. Rev. Biophys. Biomol. Struct. 25*, 259–286.
(4) Stubbe, J., Nocera, D. G., Yee, C. S., and Chang, M. C. Y. (2003) Radical initiation in the class I ribonucleotide reductase: Long-range proton-coupled electron transfer? *Chem. Rev. 103*, 2167–2202.
(5) Högbom, M., Stenmark, P., Voevodskaya, N., McClarty, G., Gräslund, A., and Nordlund, P. (2004) The radical site in Chlamydial ribonucleotide reductase defines a new R2 subclass. *Science 305*, 245–248.
(6) Jiang, W., Yun, D., Saleh, L., Barr, E. W., Xing, G., Hoffart, L. M., Maslak, M.-A., Krebs, C., and Bollinger, J. M.Jr. (2007) A manganese(IV)/iron(III) cofactor in *Chlamydia trachomatis* ribonucleotide reductase. *Science 316*, 1188–1191.
(7) Voevodskaya, N., Lendzian, F., Ehrenberg, A., and Gräslund, A. (2007) High catalytic activity achieved with a mixed manganese-iron site in protein R2 of *Chlamydia* ribonucleotide reductase. *FEBS Lett. 581*, 3351–3355.
(8) Roos, K., and Siegbahn, P. E. M. (2009) Density functional theory study of the manganese-containing ribonucleotide reductase from *Chlamydia trachomatis*: Why manganese is needed in the active complex. *Biochemistry 48*, 1878–1887.
(9) Bollinger, J. M.Jr., Jiang, W., Green, M. T., and Krebs, C. (2008) The manganese(IV)/iron(III) cofactor of *Chlamydia trachomatis* ribonucleotide reductase: Structure, assembly, radical initiation, and evolution. *Curr. Opin. Struct. Biol. 18*, 650–657.
(10) Voevodskaya, N., Lendzian, F., Sanganas, O., Grundmeier, A., Gräslund, A., and Haumann, M. (2009) Redox intermediates of the Mn-Fe site in subunit R2 of *Chlamydia trachomatis* ribonucleotide reductase. An X-ray absorption and EPR study. *J. Biol. Chem. 284*, 4555–4566.
(11) Younker, J. M., Krest, C. M., Jinag, W., Krebs, C., Bollinger, J. M. Jr., and Green, M. T. (2008) Structural analysis of the Mn(IV)/Fe (III) cofactor of *Chlamydia trachomatis* ribonucleotide reductase by extended X-ray absorption fine structure spectroscopy and density functional theory calculations. *J. Am. Chem. Soc. 130*, 15022–15027.
(12) Jiang, W., Saleh, L., Barr, E. W., Xie, J., Maslak Gardner, M., Krebs, C., and Bollinger, J. M.Jr. (2008) Branched activation- and catalysis-specific pathways for electron relay to the manganese/iron cofactor in ribonucleotide reductase from *Chlamydia trachomatis*. *Biochemistry 47*, 8477–8484.
(13) Roschick, C., Iliffe-Lee, E. R., and McClarty, G. (2000) Cloning and characterization of ribonucleotide reductase from *Chlamydia trachomatis*. *J. Biol. Chem. 275*, 38111–38119.
(14) Mann, G. J., Gräslund, A., Ochiai, E.-I., Ingemarson, R., and Thelander, L. (1991) Purification and characterization of recombinant mouse and herpes simplex virus ribonucleotide reductase R2 subunit. *Biochemistry 30*, 1939–1947.
(15) Davis, R., Thelander, M., Mann, G. J., Behravan, G., Soucy, F., Beaulieu, P., Lavallee, P., Graslund, A., and Thelander, A. (1994) Purification, characterization, and localization of subunit interaction area of recombinant mouse ribonucleotide reductase R1 subunit. *J. Biol. Chem. 269*, 23171–23176.
(16) Engström, Y., Eriksson, S., Thelander, L., and Åkerman, M. (1979) Ribonucleotide reductase from calf thymus. Purification and properties. *Biochemistry 18*, 2941–2948.
(17) Voevodskaya, N., Lendzian, F., and Gräslund, A. (2005) A stable Fe^{III}-Fe^{IV} replacement of tyrosyl radical in a class I ribonucleotide reductase. *Biochem. Biophys. Res. Commun. 330*, 1213–1216.
(18) Stoll, S., and Schweiger, A. (2006) EasySpin, a comprehensive software package for spectral simulation and analysis in EPR. *J. Magn. Reson. 178*, 42–55.
(19) Reed, G. H., and Markham, G. D. (1984) EPR of Mn(II) complexes with enzymes and other proteins. *Biol. Magn. Reson. 6*, 73–142.
(20) Von Goldhammer, E., and Zorn, H. (1974) Electron paramagnetic resonance study of manganese ions bound to concanavalin A. *Eur. J. Biochem. 44*, 195–199.
(21) Whiting, A. K., Boldt, Y. R., Hendrich, M. P., Wackett, L. P., and Que, L.Jr. (1996) Manganese(II)-dependent extradiol-cleaving catechol dioxygenase from *Arthrobacter globiformis* CM-2. *Biochemistry 35*, 160–170.
(22) Voevodskaya, N., Galander, M., Högbom, M., Stenmark, P., McClarty, G., Gräslund, A., and Lendzian, F. (2007) Structure of the high-valent Fe^{III}-Fe^{IV} state in ribonucleotide reductase (RNR) of *Chlamydia trachomatis*: Combined EPR, ^{57}Fe-, ^{1}H-ENDOR and X-ray studies. *Biochim. Biophys. Acta 1774*, 1254–1263.
(23) Cooperman, B. S. (2003) Oligopeptide inhibition of class I ribonucleotide reductases. *Biopolymers 71*, 117–131.
(24) Kjoller-Larsen, I., Sjöberg, B.-M., and Thelander, L. (1982) Characterization of the Active Site of Ribonucleotide Reductase of *Escherichia coli*, Bacteriophage T4 and Mammalian Cells by Inhibition Studies with Hydroxyurea Analogues. *Eur. J. Biochem. 125*, 75–81.
(25) Nyholm, S., Thelander, L., and Gräslund, A. (1993) Reduction and loss of the iron center in the reaction of the small subunit of mouse ribonucleotide reductase with hydroxyurea. *Biochemistry 32*, 11569–11574.
(26) Thelander, L., Gräslund, A., and Thelander, M. (1983) Continual presence of oxygen and iron required for mammalian ribonucleotide reduction: Possible regulation mechanism. *Biochem. Biophys. Res. Commun. 110*, 859–865.
(27) Henriksen, M. A., Cooperman, B. S., Salem, J. S., Li, L.-S., and Rubin, H. (1994) The Stable Tyrosyl Radical in Mouse Ribonucleotide Reductase Is Not Essential for Enzymic Activity. *J. Am. Chem. Soc. 116*, 9773–9774.
(28) Pötsch, S., Lendzian, F., Ingemarson, R., Hörnberg, A., Thelander, L., Lubitz, W., Lassmann, G., and Gräslund, A. (1999) The Iron-Oxygen Reconstitution Reaction in Protein R2-Tyr-177 Mutants of Mouse Ribonucleotide Reductase. *J. Biol. Chem. 274*, 17696–17704.
(29) Abragam, A., and Bleaney, B. (1970) Electron paramagnetic resonance of transition ions , Oxford University Press, London.
(30) Walsby, C. J., Telser, J., Rigsby, R. E., Armstrong, R. N., and Hoffman, B. M. (2005) Enzyme control of small-molecule coordination in FosA as revealed by ^{31}P pulsed ENDOR and ESE-EPR. *J. Am. Chem. Soc. 127*, 8310–8319.
(31) De Vos, D. E., Weckhuysen, B. M., and Bein, T. (1996) ESR fine strucutre of manganese ions in zeolite A detects strong

variations of the coordination environment. *J. Am. Chem. Soc. 118*, 9615–9622.
(32) Golombek, A. P., and Hendrich, M. P. (2003) Quantitative analysis of dinuclear manganese(II) EPR spectra. *J. Magn. Reson. 165*, 33–48.
(33) Yévenes, A., González-Nilo, F. D., and Cardemil, E. (2007) Relevance of phenylalanine 216 in the affinity of *Saccharomyces cerevisiae* phosphoenolpyruvate carboxykinase for Mn(II). *Protein J. 26*, 135–141.
(34) Käss, H., MacMillan, F., Ludwig, B., and Prisner, T. F. (2000) Investigation of the Mn binding site in cytochrome *c* oxidase from *Paracoccus denitrificans* by high-frequency EPR. *J. Phys. Chem B 104*, 5362–5371.
(35) Chang, C. H., Svedruzić, D., Ozarowski, A., Walker, L., Yeagle, G., Britt, R. D., Angerhofer, A., and Richards, N. G. J. (2004) EPR Spectroscopic Characterization of the Manganese Center and a Free Radical in the Oxalate Decarboxylase Reaction. *J. Biol. Chem. 279*, 52840–52849.
(36) Frausto da Silva, J. J. R., and Williams, R. J. P. (2006) The biological chemistry of the elements. The inorganic chemistry of life , 2nd ed., Oxford University Press, London.
(37) Yévenes, A., Espinoza, R., Rivas-Pardo, J. A., Villarreal, J. M., González-Nilo, F. D., and Cardemil, E. (2006) Site-directed mutagenesis study of the microenvironment characteristics of Lys213 of *Saccharomyces cerevisiae* phosphoenolpyruvate carboxykinase. *Biochimie 88*, 663–672.
(38) Andersson, C. S., and Högbom, M. (2009) A *Mycobacterium tuberculosis* ligand-binding Mn/Fe protein reveals a new cofactor in a remodeled R2-protein scaffold. *Proc. Natl. Acad. Sci. U.S.A. 106*, 5633–5638.